

A comparison of two novel approaches for conducting detect and avoid flight test

Kristopher Ellis, Iryna Borshchova, Sion Jennings, and Caidence Paleske

Abstract: This paper compares two approaches developed by the National Research Council of Canada to conduct “near-miss” intercepts in flight test, and describes a new method for assessing the efficacy of these trajectories. Each approach used a different combination of flight test techniques and displays to provide guidance to the pilots to set-up the aircraft on a collision trajectory and to maintain the desired path. Approach 1 only provided visual guidance of the relative azimuth and position of the aircraft, whereas Approach 2 established the conflict point (latitude/longitude) from the desired geometry, and provided cross track error from the desired intercept as well as speed cueing for the arrival time. The performance of the approaches was analyzed by comparing the proportion of time where the predicted closest approach distance was below a desired threshold value. The analysis showed that Approach 2 resulted in more than double the amount of time spent at or below desired closest approach distance across all azimuths flown. Moreover, since less time was required to establish the required initial conditions, and to stabilize the flight paths, the authors were able to conduct 50% more intercepts.

Key words: detect and avoid, flight test, collision volume, closest point of approach.

Résumé : Le présent document compare deux approches mises au point par le Conseil national de recherches du Canada pour effectuer des interceptions de quasi-collision en vol d'essai et décrit une nouvelle méthode pour évaluer l'efficacité de ces trajectoires. Chaque approche a utilisé une combinaison différente de techniques et de présentations d'essais en vol pour guider les pilotes afin de régler l'avion sur une trajectoire de collision et de maintenir la trajectoire désirée. L'approche 1 ne fournissait qu'un guidage visuel de l'azimut relatif et de la position de l'aéronef, tandis que l'approche 2 a établi le point de conflit (latitude/longitude) à partir de la géométrie visée, et a fourni l'écart de route de l'interception visée ainsi que des indications de vitesse pour l'heure d'arrivée. Les caractéristiques des approches ont été analysées en comparant la proportion de temps où la distance de rapprochement maximal prévue était inférieure à la valeur seuil souhaitée. L'analyse a montré que l'approche 2 a donné lieu à plus du double du temps passé à la distance de rapprochement maximal souhaitée ou en deçà dans tous les azimuts. De plus, comme il a fallu moins de temps pour établir les conditions initiales requises et pour stabiliser les trajectoires de vol, les auteurs ont pu effectuer 50 % d'interceptions supplémentaires. [Traduit par la Rédaction]

Mots-clés : détecter et éviter, vol d'essai, volume de collision, point de rapprochement maximal.

Received 18 March 2021. Accepted 15 May 2021.

K. Ellis, I. Borshchova, S. Jennings, and C. Paleske. National Research Council Canada, Ottawa, ON K1A 0R6, Canada.

Corresponding author: Iryna Borshchova (e-mail: iryna.borshchova@nrc-cnrc.gc.ca).

Copyright remains with the author(s) or their institution(s). Permission for reuse (free in most cases) can be obtained from copyright.com.

1. Introduction

The recent and rapid growth of remotely piloted aircraft systems (RPAS) underscores the urgent need for technology that will reduce the risk of mid-air collisions, enabling safer flight in the beyond visual line of sight regime. For example, RPAS with long-range and high endurance are well suited to missions such as pipeline or hydro-corridor inspection, forest fire monitoring, or persistent surveillance. These operations require a high degree of automation to be safely conducted in non-segregated and even uncontrolled airspaces. A crucial element necessary for safe remote and automated operation is a detect and avoid (DAA) capability available onboard the RPAS. The purpose of the DAA functionality is to enhance the situational awareness of the remote pilot by allowing them to see, sense, or detect conflicting aircraft, and take appropriate action to remain well-clear or avert a collision. A reversionary automatic collision avoidance capability is required in the event the remote pilot is unable to respond in a timely fashion.

The National Research Council of Canada (NRC) has been conducting research into DAA technology since 2009 and is actively collaborating with civil aviation regulators and standards bodies regarding the evaluation of candidate DAA technologies. These efforts have emphasized the need for improved methods and techniques to flight-test a DAA system. The stepped approach supported by regulatory authorities and standards bodies consisted of (i) sensor data collection; (ii) system evaluation via simulation; and ultimately, (iii) demonstration via flight test (Gahan 2019; ASTM 2020; ASTM 2021). To support flight test, there is a need to define and develop thorough in-flight validation techniques that permit the conduct of “near-miss” approaches between two aircraft at variable intercept azimuths and elevations. Only then can one examine, quantify and prove the ability to detect and avoid other traffic.

In most cases, having two aircraft arrive at a predetermined position at a chosen time, while maintaining a constant geometry, requires the solving of two simultaneous four-dimensional (longitude, latitude, altitude, and time) navigation problems. Those encounter trajectories must be simultaneously followed by both aircraft prior to the initiation of the collision avoidance maneuver. Allegorically speaking, one must solve the “detect and collide” problem to enable investigation of the DAA problem.

While there is a great body of literature investigating the DAA problem, only a small subset of articles have demonstrated flight test results (Zarrelli 1983; Glen 2003; NASA 2008; Shakernia et al. 2007; Marston and Baca 2015). Of these, even fewer sources discuss flight testing techniques required to conduct these demonstrations. The classical technique for conducting “near-miss” intercepts involves the initial point (IP) set up, which involves two aircraft departing IPs simultaneously at predefined velocities and track angles to arrive at the same location. This technique is used in several literature sources, described below.

Shakernia et al. (2007) discuss the results of testing a DAA technology, comprised of an electro-optical sensor and traffic alert and collision avoidance system (TCAS) and lessons learned from the flight test activities. The flight test scenarios were conducted using five basic conditions: level head-on, level overtake, level abeam, and descending/ascending head-on. Test geometries were set up through establishment of IPs in space for each vehicle, at which time prescribed “on conditions” were to be achieved (e.g., track, indicated airspeed, climb/descent rate). Both vehicles attempted to reach their IPs simultaneously, and on condition.

Shakernia et al. (2007) also showed that for the level head-on and level overtake scenarios, timing between the two vehicles was not particularly important; the two vehicles, if flying their prescribed tracks, will eventually meet, regardless of time. In the case when the actual location of the closest point of approach (CPA) deviated from the

planned CPA location, the test would still have been performed successfully. However, for the abeam, ascending, and descending geometries, it was critical that the planned CPA remained fixed in space. The results also suggested that winds increased the difficulty of conducting successful intercepts by requiring the pilots to apply a wind correction angle to establish the desired ground track. Variability in the wind speed and (or) direction would require the determination of new correction angles during the intercept.

NASA previously employed a flight test technique to investigate cooperative collision avoidance (NASA 2008) whereby each aircraft (ownship and intruder) departed from their IP at a time that would have them arrive at the planned CPA “simultaneously”. The ownship aircraft always used the same initial position, whereas the intruder aircraft used four IPs to generate co-heading, low-aspect, abeam, and head-on encounter geometries.

Marston and Baca (2015) presented the flight test report from the NASA Armstrong trials of the ACAS-Xu self-separation flight tests. The technique employed for these tests also involved prescribed IPs and arrival times. The intruder’s CPA was a predefined position that was 1.5, 1.0, 0.5, or 0 M distance from the remotely piloted aircraft’s position at CPA. Encounter types flown were head-on, overtake, and crossing.

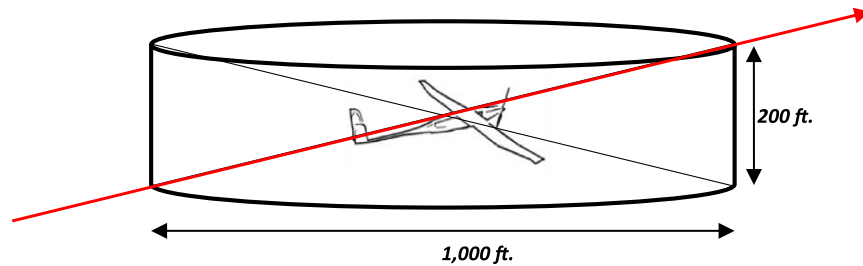
While the DAA problem is new, flight testing of air-to-air radar and other anti-collision systems on manned aircraft has been conducted for decades (RTCA 2017). For example, Zarrelli (1983) describes the results of testing TCAS and modifications of its logic. This reference stresses the challenges that can arise during the evaluation of cooperative collision avoidance systems, however neither encounter geometry design, nor flight test techniques are described in detail. Glen (2003) investigates flight testing techniques for terrain avoidance using high-performance aircraft, and considers safety altitude buffers as well as pilot display implications. The flight test description, however, is not sufficiently detailed to provide assistance in the design of a similar trial. Moreover, the described flight tests are designed for high-performance military aircraft (F-18) and the techniques are unsuitable for most small RPASs.

Based on the research conducted so far, the drawbacks of the classical IP technique are as follows:

1. The technique requires rigid planning that is not easily adapted to changes in airspace access, winds, weather, etc.
2. It is inefficient for small RPASs with limited endurance, and unnecessarily expends valuable flight test time by requiring transits to pre-planned IPs.
3. It is not accurate, since displays intended for en-route navigation of aircraft were not designed to provide course and speed guidance of sufficient precision to conduct intercepts with other aircraft.
4. There is often no direct feedback or guidance of cross track and (or) speed error provided to the pilot; typically, pilots fly fixed track angle, heading and speed, which can result in an integrated error.

NRC has been conducting DAA near miss flight testing since 2009. Two approaches for conducting collision intercepts have been developed over this time. For the purpose of this paper, an “Approach” is a combination of a flight-testing technique and a hardware configuration, including pilot displays and guidance. The initial testing (2009–2012) was done using Approach 1 (Keillor et al. 2011) but there were some issues with this approach. To address shortcomings of Approach 1, NRC developed new techniques and displays (Approach 2) to facilitate the conduct of collision intercepts from various azimuths. These approaches and the methods to assess their efficacy are described herein.

Fig 1. RPA collision volume.



This paper presents the flight test performance results by comparing Approaches 1 and 2. Section 2 describes background information on collision geometry. Section 3 describes the test hardware. Section 4 describes Approaches 1 and 2. Section 5 demonstrates the results of the data analysis when flying intercepts using the newly developed data analysis approach. Finally, the conclusions and future work are described in Section 6.

2. Collision geometry background

A near-midair collision is defined when the intruder aircraft penetrates the remotely piloted aircraft (RPA) collision volume (CV) (RTCA 2020). The CV of an aircraft is a cylindrical volume of airspace centered on an aircraft (ownship) that defines the minimum desired separation between it and another aircraft prior to the declaration of a “near-miss”. This volume, as depicted in Fig. 1, is defined as a cylinder having a horizontal radius of 500 ft and a vertical height of 200 ft (± 100 ft) which remains fixed regardless of aircraft size and model. Furthermore, the volume’s orientation is fixed, with the base of the cylinder parallel to the horizon, regardless of the aircraft attitude and or flight path.

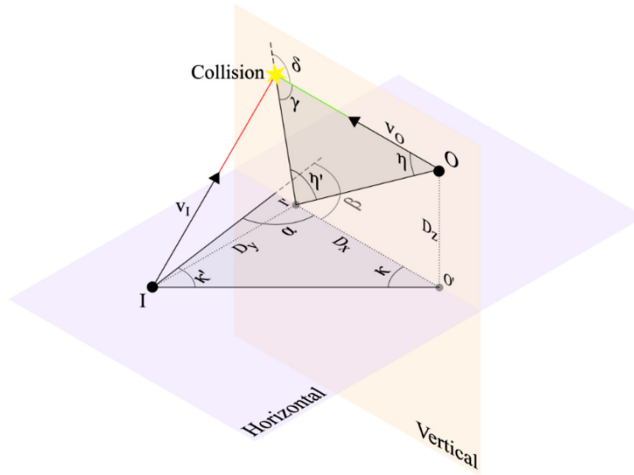
In addition to the CV, standards bodies like RTCA have actively investigated several candidate well-clear volume (WCV) definitions for en-route and terminal RPAS operations (RTCA 2020). A WCV is a desired separation between an RPA and intruder aircraft to meet the intents of FAA 14 CFR part 91, and is larger than the CV. Collision intercepts described in this paper were designed to investigate the encounters when the intruder penetrates the CV. However, it is possible to extend the developed techniques to investigate the penetration of various WCVs.

2.1. Collision geometry

Prior to discussing collision geometry, a brief discussion of terminology is warranted. This paper uses the terms “ownship” and “intruder” in multiple contexts, and some clarification is required to prevent confusion. In the context of the conduct of DAA flight test the term “ownship” refers to the remotely piloted aircraft (or surrogate), and “intruder” refers to the other participant aircraft. However in the context of the description of display guidance “ownship” refers to the reference frame as viewed from the perspective of the display symbology being drawn, and “intruder” refers to the other participant aircraft that is drawn relative to the ownship reference frame. In other words, in the context of the display symbology each pilot views their own aircraft as “ownship”, and the other aircraft as the “intruder”. For consistency we refer to all azimuths from the perspective of the remotely piloted aircraft as the “ownship”.

Collision intercepts are simultaneous four-dimensional problems; at least two aircraft must intersect in both space and time. The intersection converges into a collision course when both aircraft approach a point sufficiently close in space to penetrate the CV at time

Fig. 2. Collision geometry – qualification of relevant parameters.



$t = 0$. Figure 2 presents a generalized and simplified collision course geometry in three dimensions for non-maneuvering aircraft on stable flight paths. The intruder aircraft is represented by the point I (intruder) and the ownship aircraft is represented by the point O (ownship). Note that winds are not considered in this analysis. Collision timings and speeds are calculated based on ground speed.

The ownship and intruder velocity vectors (Fig. 2) are indicated by V_o and V_i respectively, while az and el indicate azimuth and elevation angles in the ownship reference frame. Both vectors may be multiplied by a time offset t , defined as seconds until impact, to compute the distance. This distance may be updated at each time step, the interval for which is defined by the sensor scan rate or the avoid algorithm update rate. The angles α and γ are of principal interest and can be derived from the cosine law side-side-angle equations.

The collision geometry angles can be solved for a given set of ownship and intruder ground speeds and a desired azimuth (κ' in Fig. 2). With α solved, the required initial separation distance for a 3 min collision intercept can be determined by

$$(1) \quad R_{sep} = \left(\frac{V_i \sin(\alpha)}{\sin(\kappa')} \right) (3 \text{ min} \times 60 \text{ s/min})$$

where R_{sep} is the required initial separation distance in nautical miles (M); V_i is the intruder speed in nautical miles per second (M/s).

The conflict point is represented by the intersection of the ownship and intruder velocity vectors in Fig. 2. Its location may be determined in world-referenced Cartesian coordinates (e.g., Universal Transverse Mercator, UTM) provided the initial positions of the ownship and intruder, and desired azimuth κ' are known

$$(2) \quad \text{TrackCP}_o = \text{atan2}(E_i - E_o, N_i - N_o) + \kappa'$$

where TrackCP_o is the required track angle to the conflict point for the ownship relative to true north, E_i and E_o are the eastings of the intruder and ownship (respectively) in UTM coordinates, N_i and N_o are the northings of the intruder and ownship (respectively) in UTM coordinates, κ' is the desired collision intercept azimuth, and atan2 is a four quadrant arc tangent function.

After the angle α has been solved (in degrees), κ may be easily determined by

$$(3) \quad \kappa = 180 - \alpha - \kappa'$$

Once a collision intercept run has started, the location of the conflict point must be held fixed and used as input to the guidance technology (e.g., display). Upon start of the intercept, the location of the conflict point may be determined by

$$(4) \quad \text{DistCP}_o = \frac{\sqrt{(N_o - N_i)^2 + (E_o - E_i)^2} \sin(\kappa)}{\sin(\alpha)}$$

$$(5) \quad \text{CP}_N = N_o + \sin(\text{TrackCP}_o) \text{DistCP}_o$$

$$(6) \quad \text{CP}_E = E_o + \cos(\text{TrackCP}_o) \text{DistCP}_o$$

where DistCP_o is the distance from the ownship to the conflict point in metres, CP_N is the distance from the UTM northing of the conflict point in metres, and CP_E is the distance from the UTM easting of the conflict point in metres.

3. Test hardware

The test equipment described in this section was standardized as much as possible for both Approach 1 and Approach 2. To conduct collision intercepts, one needs two aircraft which represent the ownship and intruder, as well as a sensor for position information. During these flight tests, an ADS-B system provided the positioning information. The equipment to support position sensing, cooperative aircraft detection via ADS-B, and data recording/transmission to the displays was installed on the intruder aircraft in a “seated man-rack” described in Section 3.3. A touch screen display was installed in each aircraft to present guidance to the pilot with respect to speed and position as well as allowing the test team a means to enter geometries for collision intercept. The Apple iOS development framework was used to program the display software (iCollide), and enabled the display to be executed on a smartphone on the intruder aircraft, as well as on a high brightness monitor (using the iOS simulator) on the ownship surrogate RPAS.

3.1. Surrogate RPAS – NRC Bell 205 airborne simulator

The aircraft chosen to serve as the surrogate RPAS for this investigation was the NRC Bell 205 Airborne Simulator, a single main rotor helicopter that has been extensively modified for fly-by-wire (FBW) operation (Fig. 3), (Ellis et al. 2017). The NRC Bell 205 features an experimental FBW control system, and a reversionary mechanical control system allowing a safety pilot to fly via traditional mechanical hydraulic control.

Once the safety pilot engaged the FBW system via a pushbutton on the cyclic grip, control of the aircraft was transferred to the autopilot flight control laws. The safety pilot was capable of manually disengaging the FBW system at any time in two ways: through selected disengagement via switches (the nominal method for disengagement), and by manually overriding the controls. For Approach 1, all intercepts in the Bell 205 were manually flown by the safety pilot, whereas for Approach 2 they were flown by the autopilot and included automatic collision avoidance logic.

3.2. Intruders: NRC’s harvard Mk IV, Bell 206 jetranger, extra 300, and twin otter

Four aircraft have served the role of “intruder” since the NRC began performing near-mid-air collision intercepts in 2009 (Fig. 4). These aircraft, shown in Fig. 4 clockwise from the top left, are the Harvard Mk IV, Bell 206 Jetranger, Twin Otter, and Extra 300. During Approach 1 testing, the Harvard and the Bell 206 were used as intruder aircraft to provide

Fig. 3. NRC Bell 205 Airborne Simulator.



Fig. 4. Intruder aircraft (Clockwise from top left: T-6 Harvard, Bell 206 Jetranger, DHC-3 Twin Otter, Extra 300).

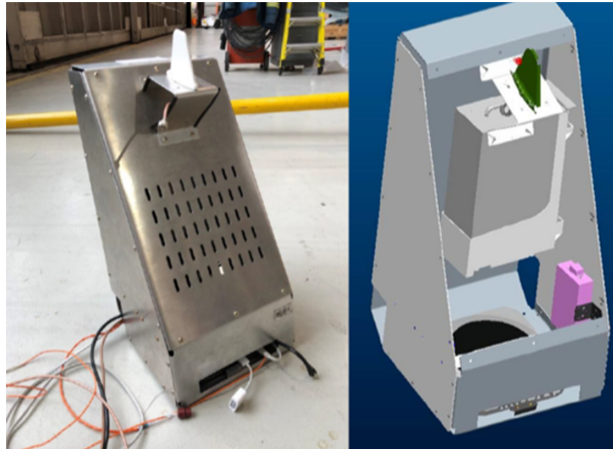


representative samples of rotorcraft and fixed wing aircraft in the 2000 lb category. The Harvard flew the intercepts at 120 kn and the Bell 206 flew intercepts at 86 kn due to speed limitations. During Approach 2 testing, the Extra 300 and Twin Otter were used, both flying at 120 kn.

3.3. Seated man-rack installation

To permit a rapid deployment of flight test instrumentation and a flexible choice of intruder aircraft, the test team developed the seated man-rack shown in Fig. 5. This

Fig. 5. Seated man-rack installation.



equipment rack was designed to be connected to aircraft power and signal systems (e.g., INS). The seated man-rack was installed in an aircraft seat, and fastened via existing aircraft seat belts. Its design evolved over the course of the project to address specific integration issues encountered on the various intruder aircraft.

4. Flight test approaches

A number of test programs examining DAA capabilities were flown at NRC from 2009 to 2019. The methods involved a combination of display software (iCollide), hardware and flight test procedures. They were broadly grouped into two categories of guidance symbology and flight test techniques that were used during this time period: Approach 1 (2009–2012) and Approach 2 (2016–2019). It is important to note the equipment limitations on the test aircraft that required the development of a novel display and a novel flight test technique. There were no flight management systems available on the NRC aircraft to support the flight test maneuvers. As a result, the iCollide display was implemented on a smart phone to support flight test conduct and to prevent actual collisions. The displays evolved throughout the testing period and a side by side comparison of the two iCollide displays is shown in Fig. 6 and symbology elements are described in Table 1. Symbology elements are identified by circled magenta letters.

The iCollide V.1 only had 1 state (State 6) implemented, as in Fig. 6. Other display states 1–5 were eventually implemented in iCollide V.2 to aid in the initial maneuver set-up, as well as provide information to the crew on automated collision avoidance algorithms that were under test (further explained in Section 4.2). These states and other important characteristics of the display such as an auto-scaling capability are shown in the attached Supplementary File video¹ “Screen recordings from a 36° azimuth intercept conducted between the Bell 205 (left side of split screen) and Twin Otter (right side of split screen)” and described in Ellis et al. (2019).

The following sections provide detailed descriptions of Approach 1 and Approach 2.

¹Supplementary data are available with the article at <https://doi.org/10.1139/jjuvs-2021-0005>.

Fig. 6. iCollide display elements state 6, V.1 (left) and V.2 (right).

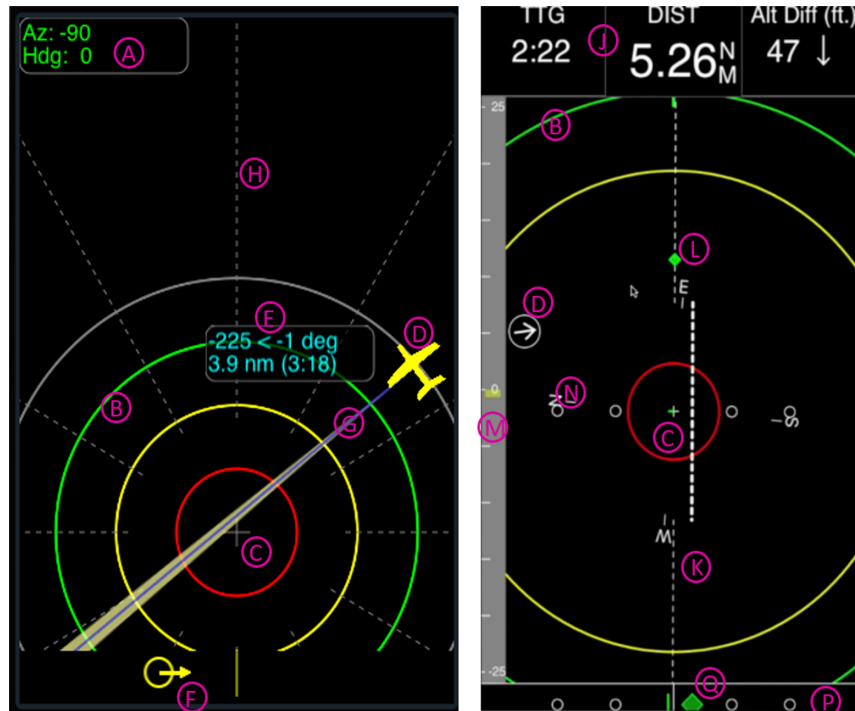


Table 1. Symbology elements for iCollide.

Symbology Element	iCollide V.1	iCollide V.2
A	Upper text dialog box	Upper text box
B	Concentric range rings	Concentric range rings
C	Ownship cross	Ownship cross
D	Intruder icon	Intruder icon with ghosted symbol
E	Text box – attached to intruder with bearing, range and time to collide information	—
F	Cross-track error ball and trend vector	—
G	Intercept beam	—
H	Background azimuth markers	—
J	—	Text box (replacing E, with time to go, range and altitude difference)
K	—	Course deviation indicator
L	—	Desired collision point
M	—	Speed guidance
N	—	Compass rose (replacement for H)
P	—	Cross track error scale
Q	—	Aircraft marker for cross track

4.1. Approach 1 (2009–2012)

For the trials using Approach 1, both aircraft were flown manually by the pilots, with the surrogate RPA pilot maintaining constant speed and track, while the pilot of the intruder aircraft was relying on iCollide V.1 display (Fig. 6) (Keillor et al. 2011). Flight test engineers on both aircraft carried test cards indicating the six collision geometry conditions (0°, -10°, -30°, -50°, -70°, and -90° azimuths) that were carried out in that order.

The flight trajectory was dependant on the selected intercept angle. The ownship (i.e., surrogate RPAS) flew on a fixed heading/track for each trial. The primary task of the intruder aircraft pilot was to acquire the appropriate beam to intercept the target relying on iCollide V.1. All flights were carried out such that each aircraft attempted to maintain a fixed ground speed throughout the trial. Speeds were decided prior to commencement of the testpoint based on intercept angle conditions. For the majority of trials, the intruder aircraft flew at 120 kn while the ownship aircraft flew at 80 kn for intercept conditions 0° , -10° , -30° , and -50° , and at 60 kn for intercept conditions -70° and -90° . Communications between ownship and intruder aircraft were carried out over a dedicated radio channel. The ownship aircraft remained in contact with ATC on another channel, while the intruder aircraft followed ownship aircraft instructions.

While the initial procedure in Approach 1 and the initial iCollide V.1 implementation showed promise, pilots reported difficulty in conducting the maneuvers during flight test. These were traced to the maneuver procedure and display deficiencies. The beam was intended to provide guidance, however it was not a compelling cue and its angular sensitivity changed with distance from the other aircraft, resulting in large course corrections at long ranges. Furthermore, while the display showed the extent of azimuthal positioning error, it did not present specific guidance to the pilot regarding how to correct for it. It was up to the pilot to decide whether to alter course or alter speed to correct the azimuthal error. Additionally, the quality of the ADS-B data was intermittent as transmissions could be blocked during dynamic maneuvers due to the fuselage blanking the ADS-B antenna, similar to the results reported in Geister and Becker (2012). The low data update rate of ADS-B would also make the aircraft symbols and guidance jerky and intermittent. Moreover, due to varying wind conditions, some trials required a wind bias as heading is not a direct indicator of aircraft track. After the initial turn in, when needed, a wind bias was called out by the ownship and entered into the iCollide V.1 of the intruder aircraft by the flight engineer. The culmination of these deficiencies resulted in the pilots abandoning use of the display once they had achieved solid visual contact with the other aircraft. The intercepts were completed on a visual basis from that point forward.

4.2. Approach 2 (2016–2019)

Approach 2 was developed to mitigate the inefficiencies of the Approach 1. Approach 2 provided a dynamic “on-the-fly” planning capability for intercept set-up in the air as well as speed and track-over-ground guidance to the intruder pilot to address the issue of the integrated error. Furthermore, Approach 2 included automatic track and speed following by the ownship surrogate RPAS, allowing the safety pilot to concentrate on visual acquisition of the intruder aircraft. For all the intercepts, both the ownship and intruder aircraft were flown based on the iCollide V.2 display (Fig. 6), which provided automatic 3D navigational guidance (latitude, longitude, and time) on how to get to the conflict point at the desired time. To support this, the following iCollide V.2 display states were implemented:

1. Configuration page.
2. Situational awareness state.
3. Geometry user entry.
4. Geometry display for determination of separation vectors.
5. Course guidance towards track to conflict point.
6. Fine track and speed guidance towards conflict point.

For brevity, this paper describes only State 6 of iCollide V.2 display. The desired track to the conflict point was indicated by the dashed white line (shown on the display in Fig. 6). The track indicator was used since it is well understood by pilots who have IFR

qualification. The central section of the display features a course deviation indicator where each white hollow dot represents 500 ft of cross track error, and the thick dashed white line represents the location of the desired ground track (e.g., in Fig. 6 the aircraft is left of track and needs to correct by a slight right turn input). A green line drawn from the ownship cross symbol represents the rate of change of the cross track error, with the sample screen capture of Fig. 6 (right) indicating that the ownship is drifting left away from the desired ground track.

Speed guidance was provided in the form of a vertical tape on the left hand side of the screen. The nominal required ground speed was determined from the distance to the conflict point divided by the remaining “time-to-go”. The current measured ground speed was then subtracted from the nominal required speed and displayed to the pilot as a bar on the tape. The overall scaling was such that 25 kn of ground speed error was full scale. The sense of the bar was such that a positive bar (upwards pointing) required the pilot to increase speed.

The cross track error and rate were re-displayed at the bottom of the screen. The only difference between these symbols and the course deviation indicator was that the course deviation symbols rotated with ownship track angle whereas the cross track error and rate symbols remain fixed to the bottom of the screen. In practice, the course deviation indicator was a more compelling and useful cue.

5. Flight test results

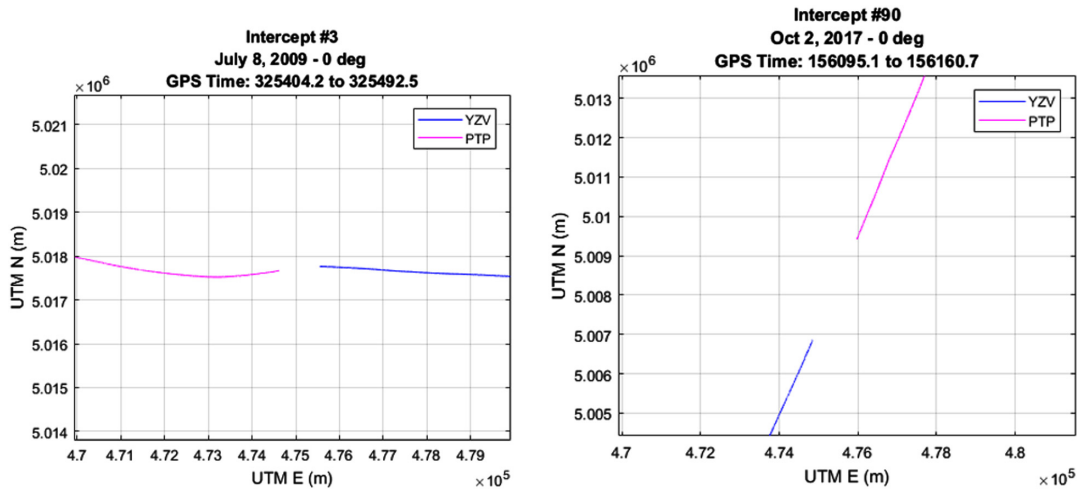
A total of 123 collision avoidance intercepts were flown between 2009 and 2019 across both techniques. Of these, 108 intercepts were considered successful, numbered chronologically, (e.g., Intercept #90), and have been included in the analyses. Unsuccessful intercepts were primarily related to equipment issues and pilot proficiency with the technique, coupled with the fact that the systems were still under development. Approach 1 was used between 2009 and 2012 for a total of 49 successful intercepts. Approach 2 was used from 2016 to 2019, with a total of 59 intercepts.

5.1. Data analysis method

Selecting an appropriate criterion for comparison of collision trajectories is a typical problem when assessing the effectiveness of the display systems and flight test maneuvers. Figure 7 presents the flight paths for two “head-on” intercepts, #3 and #90, flown in Approach 1 (left), and Approach 2 (right). By visual inspection one can see that the flight paths of Approach 2 present a higher quality intercept (the paths are aligned directionally for a longer distance and there is no curving of the path near the conflict point) than those of Approach 1, however there is no well-established quantitative metric for expressing this.

NRC’s previous attempt to assess the efficacy of Approach 1 compared the variance about the mean azimuth to the intruder as observed from the ownship surrogate RPAS (Keillor et al. 2011). An identified deficiency with this technique is that the sensitivity of the azimuth calculation is inversely dependent on distance between the intruder and ownship. Further, this approach used the azimuth relative to the ownship’s heading as the metric, as opposed to track angle. Heading has greater variability than the track angle due to the bias from wind and high frequency perturbations from aircraft dynamic modes (e.g., “Dutch roll”). While the use of azimuth relative to heading is considered appropriate for determining the location of an intruder aircraft relative to a fixed sensor mounted to the ownship (e.g., within a camera’s field of view), it is not the best measure for determining relative bearing owing to the attitude fluctuations. Additionally, the azimuth calculation does not account for the velocity vector of either the ownship, or intruder and as such tends to lag the actual dynamics that can be intuitively observed by analysis of the flight path

Fig. 7. Comparison of “head-on” flight paths using Approach 1 (left) and Approach 2 (right).



trajectories projected into a Cartesian space as shown in Fig. 7. For example, in Fig. 7 (right) at the start of the intercept the Bell 205 (YZV), and Harvard (PTP) are in a near zero azimuth condition, however visual inspection of the flight paths shows that the velocity vector of the Harvard was bringing it too far south and required a correction near the end of the intercept as can be seen by the arc in the magenta trace. While the azimuth error was low at the start of the intercept, the velocity vectors were not pointing in the right direction to achieve a near-mid-air collision.

For the performance comparison of the two approaches described in this work, a novel metric has been established that depends on the predicted CPA over the duration of the intercept. This method involved using both the position and velocity of the ownship and intruder aircraft, and using linear geometry to estimate the instantaneous closest approach distance (RTCA 2020). The estimated closest approach distance is calculated as follows:

$$(7) \quad d_{CPA} = |P_o(t_{CPA}) - P_i(t_{CPA})|$$

where P_o and P_i are ownship and intruder positions projected to the time of CPA.

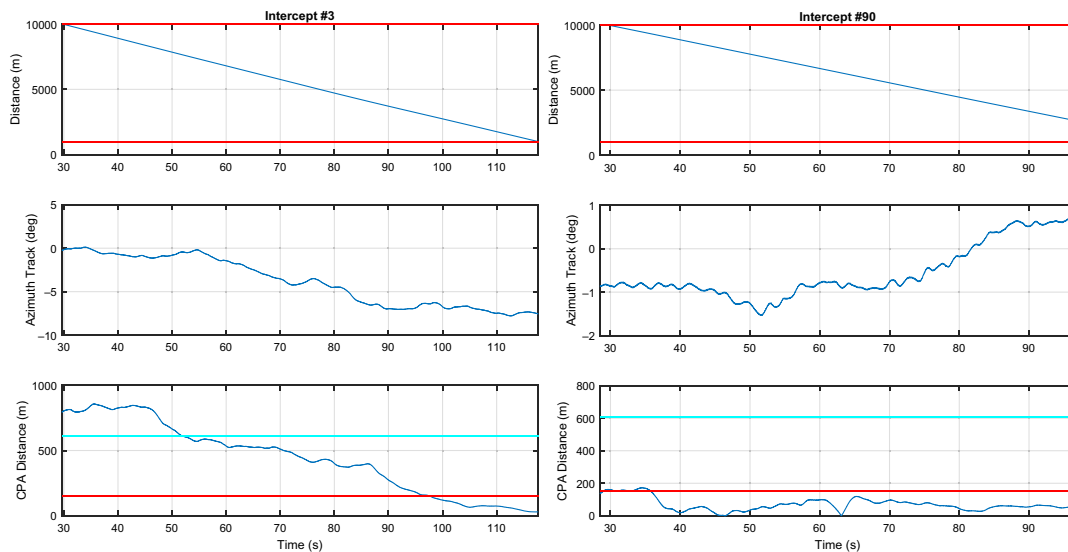
To facilitate analysis, three different threshold ranges were identified for d_{CPA} as described in Table 2. All intercepts for the flight trials described in this paper were attempting to achieve trajectories with predicted closest approach distances of <500 ft, in accordance with the conventionally understood definition of a “near miss”, and this forms the first threshold (i.e., “desired” performance). A second threshold was established at 2000 ft, which corresponds with the FAA’s proposed definition for “well clear” for small unmanned aircraft (FAA 2019), and can be considered as “adequate” performance).

It is important to note that d_{CPA} represents an instantaneous estimate of the closest approach distance, and is in fact a time series variable that must be computed over the duration of an intercept. To facilitate comparison, a consistent scheme for determining the start/end of each intercept was required. For the analysis presented in this paper, the analysis of the intercept performance was started at a separation distance of 10 km, and was terminated at a distance of 1 km, or whenever automatic avoidance was initiated; whichever came first.

Figure 8 presents a sample analysis time-history (the abscissa is time in seconds) for the 0° intercepts shown in Fig. 7 (Intercepts #3 and #90). The top plots present the separation

Table 2. Closest point of approach thresholds.

Level	Threshold d_{CPA}	Description
1 – “Desired”	≤ 500 ft (152.4 m)	At the current time the aircraft are predicted to pass within < 500 ft of one another.
2 – “Adequate”	≤ 2000 ft (609.6 m)	At the current time the aircraft are predicted to pass within < 2000 ft of one another. This is below the FAA’s proposed definition of “Well Clear” for small unmanned aircraft.
3 – “Miss”	> 2000 ft (609.6 m)	At the current time the aircraft are predicted to miss by > 2000 ft.

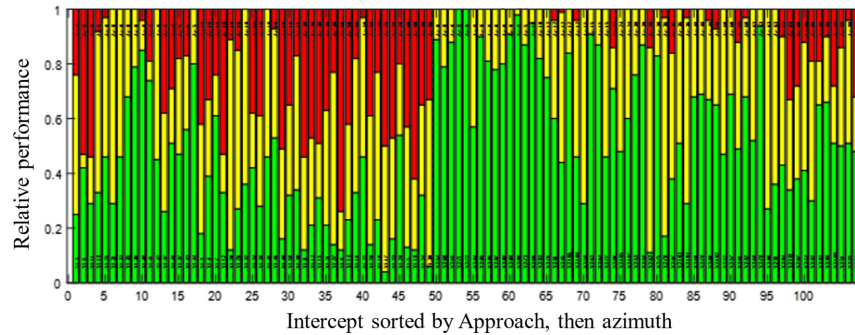
Fig. 8. Example time-history analysis of Intercepts 3 and 90, which correspond to flight paths shown in Fig. 7.

distance (in metres) between the intruder (Harvard), and the ownship. Red horizontal lines are drawn at 10 km, and 1 km to assist in determining the appropriate time ranges for data analysis. The middle plots show the azimuth from the host’s velocity vector (track) relative to the intruder (i.e., azimuth). The bottom plots present the instantaneous d_{CPA} (in metres) as calculated using the method described above. The red horizontal lines represent threshold 1–“within the collision volume” (desired), whereas the cyan lines represent threshold 2–“within the well clear volume” (adequate), as per Table 2.

Intercept #3 in Fig. 8 (left) began at the nominal 0° azimuth condition, however with a predicted d_{CPA} outside of a “well clear” miss. This implies that the velocity vectors of the host and intruder were not appropriate for establishing a near-mid-air collision. Looking at the d_{CPA} plot one can see three sections. Up until time 47 s the d_{CPA} remains relatively constant, implying that there has been little change in the relative velocity vectors. After this time, there is a gradual drop in d_{CPA} implying that some corrective action was performed, however it was not completely effective since d_{CPA} appears to flatten 53 and 85 s. Finally, there is a sharper drop in d_{CPA} at 87 s implying that a more significant corrective action had taken place. This corrective action can be seen as the arc in the magenta flight path of Fig. 7 (left).

The lower plots of Fig. 8 summarize the percentage of time spent with d_{CPA} in each threshold level. For the plot of Fig. 8 (left) this yields 25% within Level 1 – “Desired”

Fig. 9. Intercept performance bar charts sorted by approach type and then azimuth.



($d_{CPA} < 500$ ft), 51% within Level 2 – “Adequate” ($d_{CPA} > 500$ ft and < 2000 ft), and 23% within Level 3 – “Miss” ($d_{CPA} > 2000$ ft). For the plot of Fig. 8 (right) this yields 98% within Level 1 – “Desired” ($d_{CPA} < 500$ ft). This performance data can be presented in the form of a stacked bar chart presenting the proportion of the intercept spent at each d_{CPA} threshold.

5.2. Data processing results

Figure 9 presents stacked bar charts as ordinals indicating the relative performance achieved for each of the 108 successful intercepts conducted to date. The bar charts present the proportion of time spent with a d_{CPA} within each of the three thresholds identified in Table 2, with green (bottom), yellow (middle), and red (top) representing desired, adequate, and miss performance levels respectively in Fig. 9. Ordinal 50 marks the change from Approach 1 to Approach 2. The intercepts were subsequently sorted by azimuth (e.g., “head-on” azimuths for Approach 1 can be found in intercepts 1–15, and for Approach 2 in intercepts 50–62). Intercepts #3 and #90 from Figs. 7 and 8 appear as Ordinals 1 and 61 respectively. It is readily apparent from Fig. 9 that the proportion of time spent a CPA > 2000 ft is greatly reduced with Approach 2 owing to the diminished amount of red bars in the ordinals numbered 50 and higher.

The bar charts of Fig. 9 also demonstrate that there appears to be a relationship between the performance of the intercept and the azimuth; with higher azimuths generally having lower performance. Since the intercepts were collected from a variety of flight tests with different objectives, the desired azimuth angles of each test were not consistent and the data does not provide a balanced set of azimuths within the two technique/display conditions. To improve the comparison, a method was needed to group the data according to azimuth and a cluster analysis was performed to group the data.

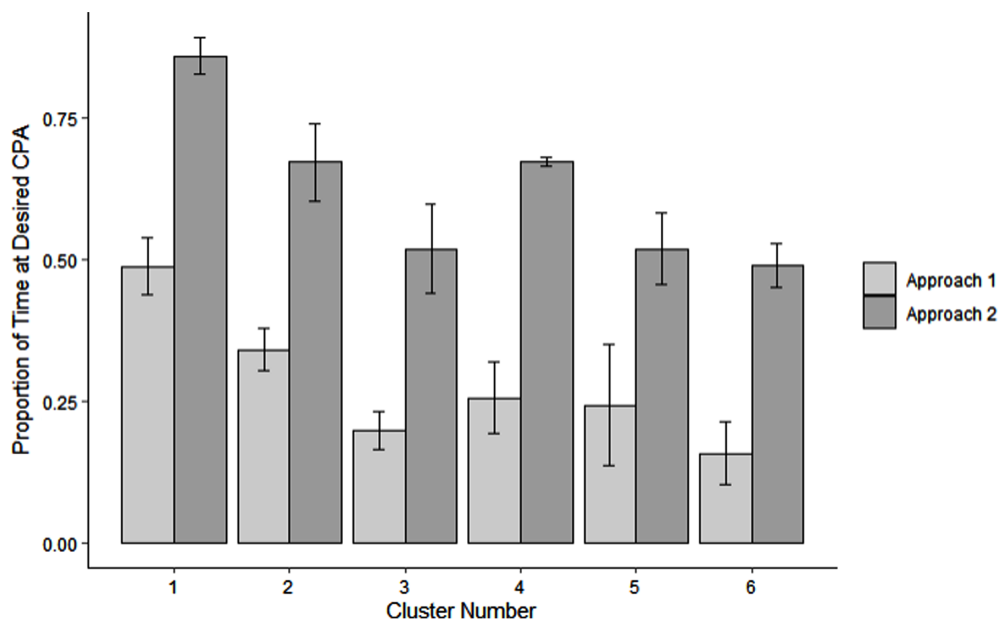
5.2.1. Grouping of azimuth performance using a cluster analysis

A cluster analysis was performed to establish groups of azimuths to facilitate the comparison between Approach 1 and 2. The optimal number of clusters was determined by examining the total within cluster variance as a function of the number of clusters – between three and eight. The optimal number of clusters in this dataset was six, as greater granularity (i.e., more clusters) did not result in significant changes of within cluster variance. Table 3 presents azimuths and number of observations for the six clusters identified in the analysis.

Figure 10 presents the average proportion of time spent at desired CPA, grouped by cluster and approach method. A higher proportion of time spent in the desired CPA therefore indicates better performance. Cluster 1 (azimuths 0° and 5°) has the highest proportion of time spent at $d_{CPA} < 500$ ft, in both Approach 1 and Approach 2, which is expected since it

Table 3. Azimuth clusters used in the analysis of Approach 1 vs. Approach 2.

Centroid	Azimuths (°)	Number of observations (Approach 1, Approach 2)
1	0, 5	31 (18,13)
2	10, 12, 15	25 (14,11)
3	24, 30, 36	16 (5,11)
4	48, 50	9 (5,4)
5	60, 63, 70	14 (4,10)
6	88, 90	13 (4,9)

Fig. 10. Average proportion of time spent at d_{CPA} , grouped by cluster and approach.

is a near head-on azimuth, and speed error is less of a factor owing to the required flight paths being nearly coincident.

It can also be seen from the Fig. 10 that performance more than doubled on average when comparing Approach 1 and Approach 2, across all azimuths flown. To statistically quantify the improvement between Approach 1 and Approach 2, a linear multivariate regression analysis was completed. Inspection of the dataset for skewedness using a Shapiro-Wilks test, as well as visual inspection, revealed deviations from a normal distribution. However, multivariate regression (Draper 1998) can still be used, so long as the error residuals around the estimation of the linear fit are normally distributed. Using ordinary least squares estimation, a linear model was created using “desired” d_{CPA} as the outcome variable, and approach version and azimuth as predictors. This model was significant ($R^2 = 0.482$, $F(2,105) = 48.82$, $p < 0.0001$), and revealed that approach methodology significantly impacted the proportion of time spent at d_{CPA} . Approach 2 resulted in more than a doubling in the amount of time spent at or below desired CPA, across all azimuths flown ($\beta = 0.325$, $SE = 0.037$, $t(107) = 8.84$, $p < .0001$). As an example, the predicted proportion of time spent at desired CPA for a 0° azimuth in Approach 2 is approximately 76.1%, compared

to 43.6% for Approach 1. Results also revealed that as azimuth increases, the amount of time spent at d_{CPA} tends to decrease ($t(107) = -6.06, p < .0001$), but that this was a fairly consistent trend across both Approach 1 and Approach 2. Pearson correlation coefficients were also computed, and support the conclusion that Approach 2 resulted in more time spent on a collision track compared to Approach 1 ($r = 0.55, p < .001$), and that smaller azimuths tend to have more time spent at d_{CPA} ($r = -0.31, p < .01$).

5.3. Intercept efficiency

One of the design goals associated with Approach 2 was to provide the test pilots with improved situational awareness regarding how to set up for the next test point in effort to increase the total number of intercepts that could be conducted within a single flight. The average number of intercepts per flight hour using Approach 1 was 3, which is the same efficiency achieved by NASA in [Marston and Baca \(2015\)](#) using the classical IP technique. Using Approach 2, NRC was able to increase the amount of intercepts per flight hour to 4.5; a 50% improvement.

6. Conclusions

To evaluate the acceptability and performance of airborne DAA systems in flight test, it is necessary to be able to conduct predictable and repeatable “near-miss” trajectories between two aircraft at various azimuths and elevations. Classical methods to conduct collision intercepts require both aircraft depart from predefined IPs at the same time and establish track/speed towards a predefined conflict point. The main drawback of such technique is that it requires rigid planning and is not easily adapted to changes in airspace availability, winds, weather and other variations in test conditions. Moreover, at the time of this paper, methods to assess efficacy of conducting such intercepts have not been presented in literature sources in detail.

Over the course of its research into DAA, NRC developed two approaches for conducting collision intercepts, which were compared in this paper. The approaches included a combination of flight test technique and required hardware, including displays. Both approaches relied on using displays (iCollide V.1 and V.2) to guide the pilot while conducting collision intercepts. While iCollide V.1 did not provide direct guidance to the pilot, iCollide V.2 calculated the conflict geometry and conflict point from the desired geometry, and displayed cross track error from the desired intercept as well as speed cueing for the arrival time.

The data processing results show that Approach 2 resulted in approximately double the amount of time spent at or below desired CPA, across all azimuths flown. A further benefit of Approach 2 was that more intercepts were able to be conducted within any given flight hour, since less time was required to establish the required initial conditions, and to stabilize the flight paths. The average number of intercepts per flight hour using Approach 1 was 3, which is the same efficiency achieved by NASA in [Marston and Baca \(2015\)](#) using the classical IP technique. Using Approach 2, NRC was able to increase the amount of intercepts per flight hour to 4.5; a 50% improvement.

NRC intends to continue improving upon Approach 2 to conduct DAA research. Planned improvements include:

1. Improved ground speed cueing to increase accuracy of co-altitude collision trajectories.
2. Vertical speed cueing and altitude guidance to enable collision trajectories that involve climbing and descending flight paths.
3. Display element tuning (e.g., cross track error scaling sensitivity) to the flight dynamics of the platform to optimise pilot tracking and reduce track, speed and altitude errors.

Acknowledgements

The authors thank Stephan Carignan and Bryan Carrothers for their guidance and for steadfastly piloting the Bell 205, and Tim Leslie, Anthony Brown, Malcolm Imray, Paul Kissman, and Rob Erdos for flying as intruder pilots. The dedication, expertise, and skill of these pilots greatly contributed to the success of this investigation as well as the safe conduct of over 120 near mid-air collision intercepts.

References

- ASTM. 2021. New Test Method on Detect and Avoid (under development). ASTM International.
- ASTM. 2020. Standard Specification for Detect and Avoid System Performance Requirements. ASTM International.
- Draper, N. 1998. Applied Regression Analysis. Wiley Series in Probability and Statistics.
- Ellis, K., Gubbels, A., and Imray, M. 2017. NRC Bell 205 FBW Systems Description in ATA-100 Format, LTR-FRL-2014-0041, National Research Council of Canada, Ottawa.
- Ellis, K., Paleske, C., Jennings, S., and Carrothers, B. 2019. Development and Flight Test of a Near Mid-Air Collision Intercept and Avoid Display. National Research Council of Canada, Ottawa.
- FAA. 2019. AC 90-WLCLR, Well Clear Definition for Small Unmanned Aircraft Systems Operating Beyond Visual Line of Sight. FAA.
- Gahan, K. 2019. Multi-Path Automatic Ground Collision Avoidance System for Performance Limited Aircraft with Flight Tests: Project Have Medusa., Thesis for Master of Science in Aeronautical Engineering. Air Force Institute of Technology.
- Geister, R., and Becker, H. 2012. Murphy's law squared – flight testing of automated closely spaced parallel approaches. Available from <https://www.semanticscholar.org/paper/MURPHY%E2%80%99S-LAW-SQUARED-FLIGHT-TESTING-OF-AUTOMATED-Geister-Becker/b6fafd405e3460ccd09b57370a9474ad6585f9c1> [accessed 26 May 2021].
- Glen, G. 2003. An Investigation of Terrain Avoidance System Flight Test Techniques for High Performance Aircraft. M.Sc.thesis, University of Tennessee.
- Keillor, J., Ellis, K., Craig, G., Rozovski, D., and Erdos, R. 2011. Studying Collision Avoidance by Nearly Colliding: Flight Test Evaluation. Proc. Hum. Factors Ergon. Soc. Ann. Meet. 55(1): 41–45. doi:[10.1177/1071181311551009](https://doi.org/10.1177/1071181311551009).
- Marston, M., and Baca, G. 2015. ACAS-Xu/Initial Self Separation Flight Tests – Flight Test Report. NASA Armstrong Flight Research Center.
- NASA. 2008. Cooperative Collision Avoidance Technology Demonstration Data Analysis Report. Report No. DFRC-239. NASA.
- RCTA DO-365. 2020. MOPS for Detect and Avoid Systems. RCTA, Inc.
- RCTA DO-366. 2017. MOPS for Air-to-Air Radar for Traffic Surveillance. RCTA, Inc.
- Shakernia, O., Chen, W-Z., Graham, S., Zvanya, J., White, A., Weingarten, N., and Raska, V. 2007. Sense and Avoid (SAA) Flight Test and Lessons Learned. In AIAA Infotech@Aerospace 2007 Conference and Exhibit, Rohnert Park, California. doi:[10.2514/6.2007-3003](https://doi.org/10.2514/6.2007-3003).
- Zarrelli, L. 1983. Performance of the Collision Avoidance Logic during Preliminary Flight Tests of the Traffic Alert and Collision Avoidance System (TCAS II). The MITRE Corporation.